BULETINUL INSTITUTULUI POLITEHNIC DIN IAŞI
Publicat de
Universitatea Tehnică „Gheorghe Asachi” din Iaşi
Volumul 72 (76), Numărul 1, 2026
Secţia
ŞTIINŢA ŞI INGINERIA MATERIALELOR

A REVIEW OF THE CURRENT STATE OF RESEARCH ON WIRE DRAWING

BY

COSTEL JIPA* and DORIN LUCA

“Gheorghe Asachi” Technical University of Iaşi, Romania

Received: January 9, 2026
Accepted for publication: February 20, 2026

Abstract. Wire drawing is one of the most popular technologies for obtaining finished products, which are then used in all industrial production sectors, from the household appliance, automotive, food, and construction industries to the aeronautical field. Parallel to the development of new wire drawing techniques, numerical and empirical approaches are being developed to improve existing methods and develop new wire drawing technologies. Many innovative numerical algorithms, experimental methods, and theoretical contributions have recently been proposed by researchers in the field. These methods are mainly focused on improving the deformability of materials, obtaining wires with increased mechanical strength, good surface quality, and minimal residual stresses, accelerating the production cycle, reducing the number of operations, and improving the environmental performance of production. The purpose of this study is to summarize recent development trends in both the numerical and experimental fields of conventional wire drawing methods, as well as in the field of new severe plastic deformation (SPD) wire drawing methods. Particular attention was paid to the period 2015-2025 regarding the progress in the development of methods for drawing difficult-to-process materials for automotive and aircraft applications, tribological aspects that have become a subject of great attention, and the assessment of the ecological impact of wire drawing processes.

Keywords:drawing, wires, severe plastic deformation, properties, structure.

*Corresponding author; *e-mail*: costel.jipa@student.tuiasi.ro

1. Introduction

Wire drawing is a plastic deformation technology that consists of passing the metal semi-finished product through dies with calibrated holes to reduce its cross-section, which will simultaneously produce the equivalent elongation of the wire based on the law of constant volume (Badi *et al.*, 2024). The main disadvantage of wire drawing is friction at the interface between the die and the material being deformed, which causes uneven deformation and, consequently, uneven properties of the drawn product in cross section.

SPD methods have proven to be powerful tools for improving and adapting the mechanical and functional properties of materials. Processing high-performance materials requires a fundamental understanding of process-structure relationships. Crystal fragmentation and structure refinement during plastic deformation occur not only during SPD processing, but also during other cold working processes, such as rolling or drawing. The introduction of dislocations into the crystal lattice, followed by their progressive rearrangement, causes fragmentation and refinement of the initial crystals. This process manifests itself in a gradual reduction in the size of the dislocation cells and a corresponding increase in their degree of disorientation as the level of applied deformation intensifies (Renk *et al*., 2024). Carbon steel wires have been significantly improved in recent years in terms of strength and ductility. A major problem with high-strength steel wires is their tendency to become brittle when they absorb hydrogen. In the case of carbon steel wires, heat treatment, chemical composition, or cold deformation may influence strength, and one of the most commonly used methods for increasing wire strength is die drawing (Truschner *et al.*, 2023*)*. Significant energy losses caused by internal and external friction, plastic changes generated by the deformation pattern, and reduced heat dissipation intensity in the deformation zone limit the increase in drawing speeds and productivity. The increase in pressure at the entrance to the die channel is determined by the effect of hydrodynamic friction of the lubricant on the moving wire. It is known that only 2.5% of the heat released in the deformation zone is dissipated directly through the die, and another 2.5% is taken up by the lubricant; thus, the remaining 95% of the energy contributes to the heating of the processed wire (Kuznestov *et al.*, 2023; Suliga *et al*., 2023; Demin and Grebenkin, 2024).

The steel wire market is expected to reach US$123.23 billion by 2031 from US$77.47 billion in 2023; and is anticipated to register a compound annual growth rate of 6.0% during the forecast period. The compound annual growth rate is the average annual growth rate of an investment over a given period of time, greater than one year. The global steel wire market has experienced significant growth due to the growth of the global automotive industry. In November 2021, the US government approved a $1.2 trillion infrastructure bill to help federal investment in various infrastructure projects.

Construction spending was also estimated to grow by 5.5% in 2023. Such government infrastructure projects involving the construction of roads, bridges, railways, and other urban development initiatives create demand for construction materials. Increased investment by government organizations leads to significant infrastructure improvements, such as the construction of roads, bridges, tunnels, ports, airports, and highways. Thus, growing investment in infrastructure projects has also led to growth in the construction industry, which ranks first in the steel wire market (**a, 2025).

Steel wire is widely used to manufacture steel wire mesh, steel wire rope, and other products. It is manufactured from several grades of carbon, alloy, and stainless steels. Carbon steel wire is produced by drawing hot-rolled bars and then through smaller dies. The drawing process has the effect of increasing the strength of the steel. Alloy steel contains alloying elements such as manganese, chromium, nickel, molybdenum, and vanadium in addition to carbon. Stainless steel is a corrosion-resistant material with high durability. Stainless steel wires are extremely adaptable for various applications as they are available in various sizes and shapes.

The steel wire segment with a diameter between 0.8 mm and 1.6 mm held the largest global market share in 2023. Steel wire with a thickness between 0.8 mm and 1.6 mm offers the best balance between strength and flexibility. It is used in various industries due to its versatile mechanical properties (**b, 2025). The basic metal coatings applied to the surface of wires include zinc, copper, brass, and nickel coatings. In the case of galvanizing, the most common methods globally are hot-dip galvanizing, electrolytic galvanizing, and thermodiffusion galvanizing. Hot-dip galvanizing is used for wire rods and wires with diameters greater than 1 mm. The thickness of the coating depends on the diameter of the product and typically varies between 10 and 70 μm.

The evolution of aluminum production between 2014 and 2024 in the seven most important regions of the world: China, South America, North America, Oceania, Africa, Asia (excluding China), Russia, and Eastern Europe is shown in Fig. 1.

Fig. 1a shows production between 2014 and 2024: 186,194 thousand tons of aluminum excluding China, and Fig. 1b shows production between 2014 and 2024: 588,521 thousand tons of aluminum including China (**c, 2025). In 2023, total global copper production was approximately 26.5 million tons. This was the highest record reported since the beginning of the century and an increase of 4.9% over the previous year. From 2000 to 2023, copper production increased by approximately 12 million tons (Fig. 2).

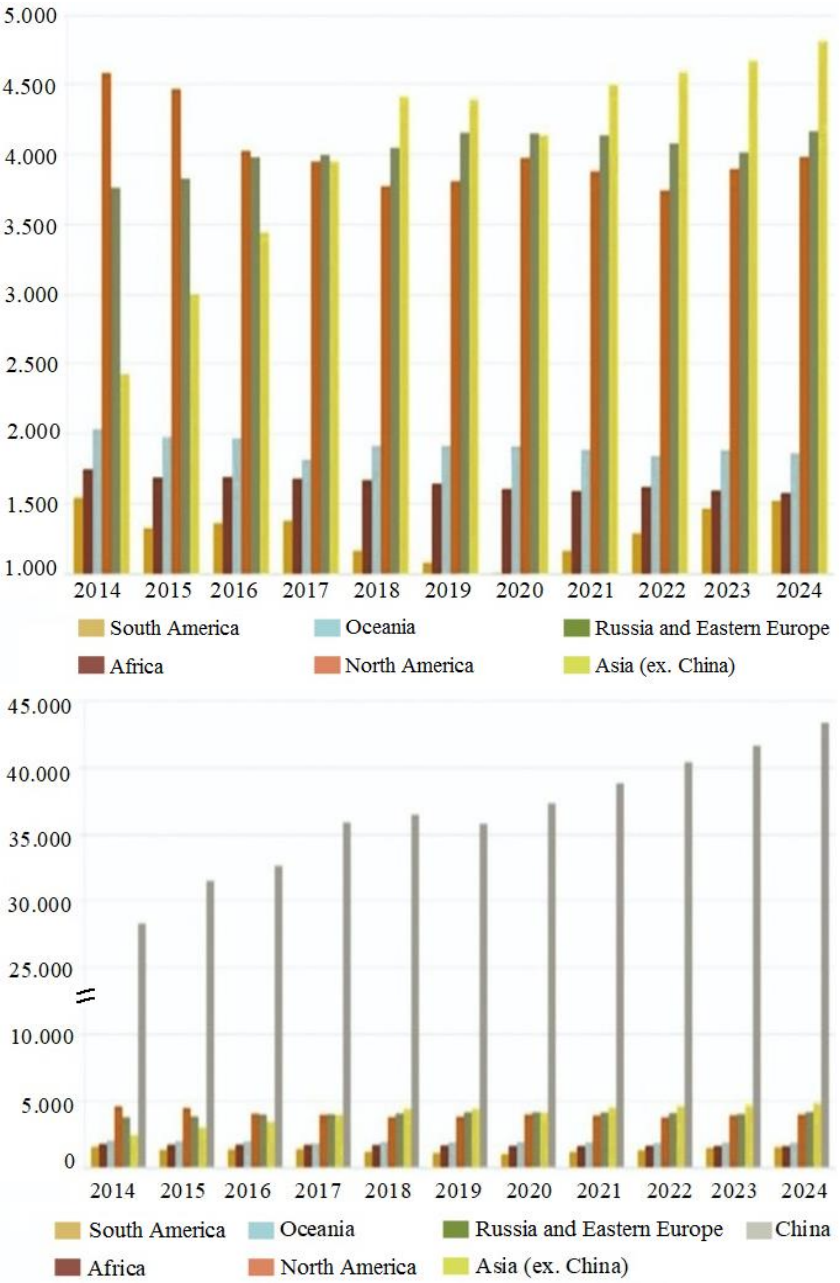

Fig. 1 – Aluminum production trends for 2014–2024:
a) excluding China; b) including China.

The dimensions of drawn wires vary depending on their intended applications and the material from which they are made. For steel wires, the usual drawing dimensions range from 0.1 mm to 12 mm, and for bars, they can reach up to 50 mm in special cases. For copper and aluminum wires, the usual drawing sizes vary between 0.1 mm and 10 mm. The lengths of drawn wires vary depending on the desired diameter and the characteristics of the working machines (*** d, 2025).

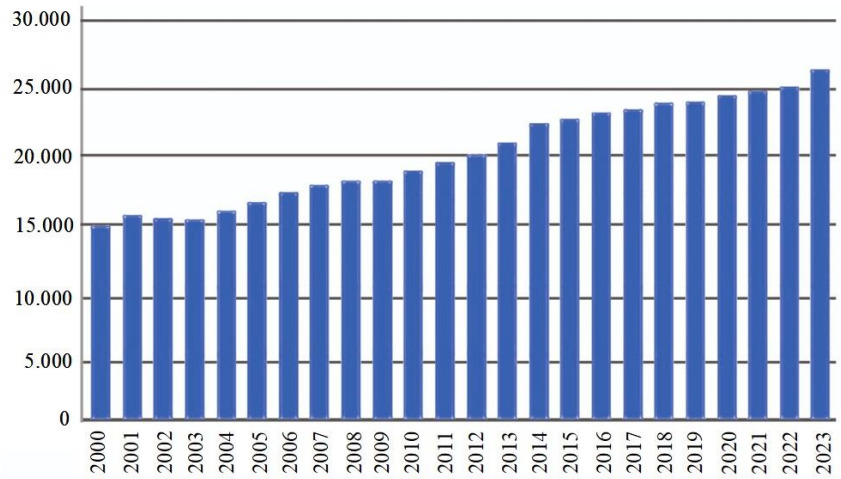

Fig. 2 − Global copper production from 2000 to 2023

2. New drawing technologies

In wire drawing processes, much attention has been paid to the deformation of very hard materials with low plasticity. These materials, when deformed in the conventional manner, cause various technological problems, such as excessive tool wear, scratches and cracks on the surface, and deviations from the circularity of the product. Therefore, there is a continuous search for technology for manufacturing very thin wires (less than 0.1 mm in diameter) from steel or alloys with low plasticity.

One of the solutions developed to address this problem is the introduction of a cumulative angular wire passing operation prior to the drawing operation. The essence of this method consists in passing the wire through a system of three arched passing dies, whose mutual arrangement of axes can be modified in a controlled manner. As a result of the passing process, shown schematically in Figure 3, a significant and uneven accumulation of deformation can be observed as the drawn material undergoes plastic deformation. This is a direct result of flow through dies, bending, and twisting.

The greatest total equivalent strain occurs in the surface layers, gradually decreasing toward the axis of the product.

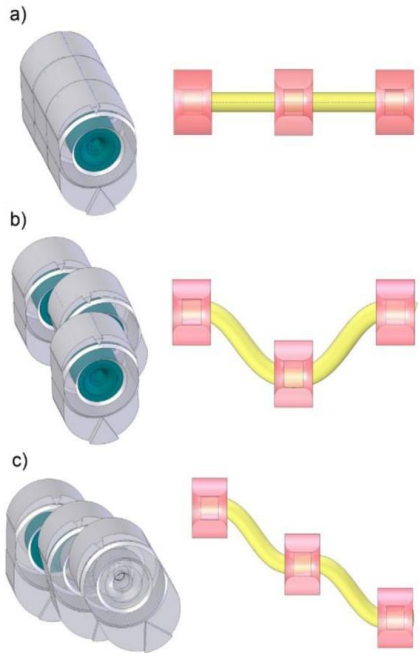

Fig. 3 – Different ways of arranging the passage dies:
a) linear; b) crank type; c) in steps.

The cumulative angular drawing process produces a material with a significantly non-homogeneous distribution of properties in the cross-section. At the same time, after deformation, the material has a high accumulated plastic deformation energy. As a result, the material that undergoes annealing after drawing has a fine grain structure in the cross section. Proper selection of the parameters of the cumulative angular drawing process makes it possible to obtain a product with high strength and good plastic properties (Gronostajski *et al*., 2019).

A recently developed method in the field of wire drawing, shown in Fig. 4, has been named the equal channel angular pressing (ECAP) and wire drawing method.

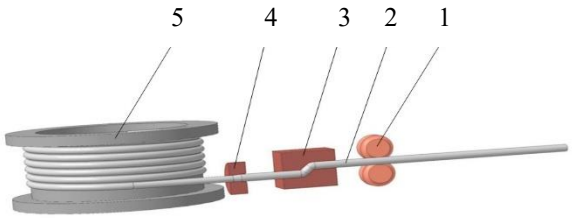

Fig. 4 – ECAP method: 1-guide roller; 2-wire; 3-die with equal angle channels; 4-die; 5-winding drum.

Experimental tests showed that the microstructure of the steel-aluminum bimetallic wire changed during plastic deformation using this method. The deformation was performed at room temperature in two passes, and it was shown that the strength properties of the wire, even after two deformation passes, increase significantly compared to the initial state: the tensile strength (σ_f) increases from 370 MPa in the initial state to 690 MPa after the second pass, and the yield strength ($\sigma_{0.2}$) increases from 260 to 465 MPa after the second pass (Volokitina *el al.*, 2023).

Another method being studied is a combination of conventional wire drawing and die-less drawing, which can reduce the wire diameter below the value that can be achieved with conventional die-only drawing technology. This new combined technology allows for a significant reduction in wire diameter and facilitates large-scale, economical production of ultra-thin wires. In addition, based on the classic wire drawing and die-less wire drawing processes, a brass wire with a diameter of 0.017 mm has been manufactured. Six times thinner than a human hair, it is believed to be the thinnest long brass wire ever manufactured in the world. The die-free drawing process was first proposed by Weiss and Kot (1969). This process is based on stretching the moving wire while simultaneously heating its plastic deformation zone (i.e., the wire is moved through a heating device so that its entire length is processed). An electric furnace, an inductor, or a laser can be used as heating devices. Adjusting the parameters of the die-less drawing process allows the production of wires with a variable diameter along their length. This is not possible in conventional drawing or extrusion processes. On the other hand, imprecise control of process parameters prevents the production of wire with a constant diameter. An important advantage of the die-less drawing process is the absence of the precise and time-consuming operation of inserting the tip of the wire (i.e., the workpiece) into the die, as in the die drawing process. This is particularly important for ultra-thin wires with a diameter of less than 0.3 mm. Another significant advantage of the die-less drawing process is the relatively high machinability in a single pass, due to the high deformation temperature and the lack of friction between the die and the wire, which means that die-less drawing

technology is more suitable than die drawing for the production of small diameter wires.

The dedicated, customized, computer-controlled machine used for drawing with and without dies is shown in Fig. 5.

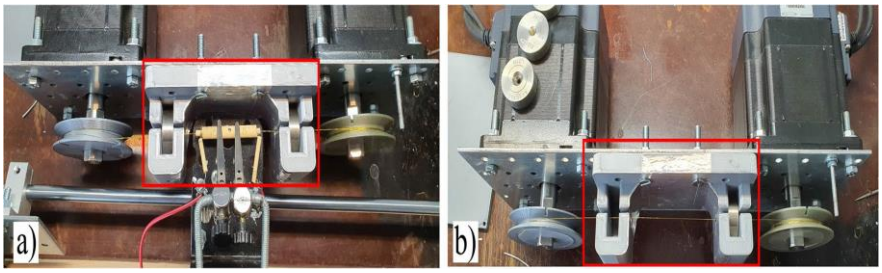

Fig. 5 – View of the experimental setup: a) drawing without a die; b) drawing with a die.

The die drawing process was performed at a drawing speed of 15 mm/s, with solid soap used as a lubricant, the reduction in cross-section in a single pass was approximately 17%, and the die angle was 12°.

A schematic representation of the processes applied is shown in Fig. 6. The process consisted of three types of wire drawing programs.

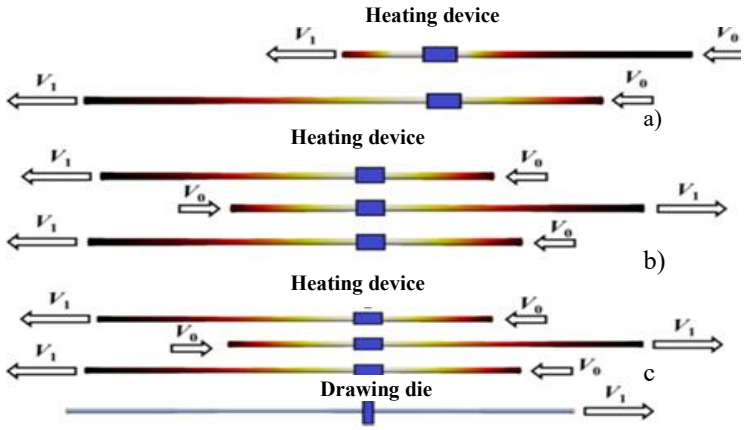

Fig. 6 – Schematic representation of applied processes: a) a single dieless pass; b) multiple dieless passes; c) a conventional pass (with a die) performed after every two dieless passes.

The first program consisted of single-pass die-less drawing as shown in Fig. 6a, and the second was a multi-pass die-less drawing program with a small partial deformation in each pass, as shown in Fig. 6b. This deformation process was controlled by a precise selection of the wire speed on both sides of the heating device (i.e., v_1 and v_0), adjusted by the rotation speed of the stepper

motors. The values of speeds v_0 and v_1 were 15 mm/s and 16.4 mm/s, respectively. The third drawing program, shown in Fig. 6c), was a combined process in which conventional drawing was applied after every 2 passes without a die. In addition, the die drawing process was used to obtain wire with a diameter of 0.02 mm. The drawing process was performed with 25 dies, then the die drawing process was performed to test the capabilities of this method.

The microscopic examination shown in Fig. 7 was performed to analyze the differences in the surface appearance of the processed wires.

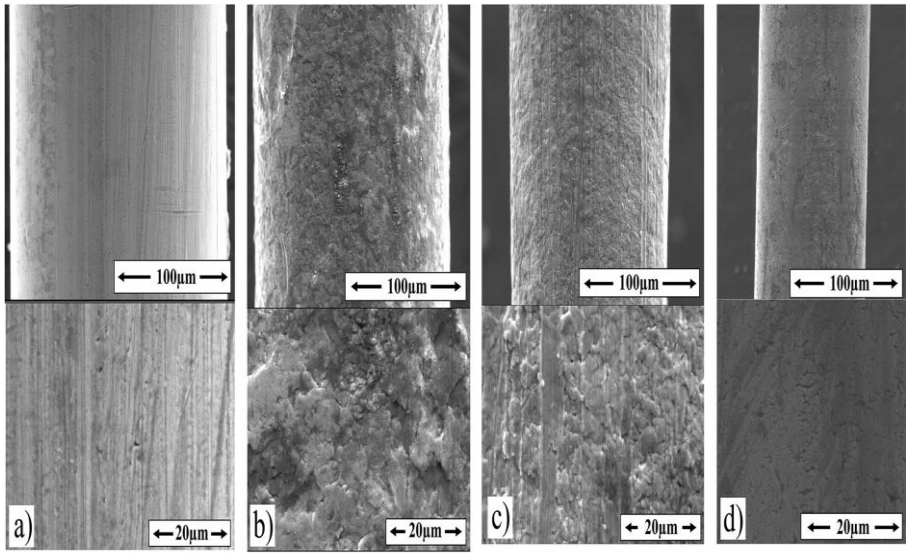

Fig. 7 – CuZn37 alloy wire: a) initial wire, d = 0.2 mm, b) after die-less drawing, d = 0.161 mm; c) after combined die-less and die drawing, d = 0.145 mm; d) after the combining drawing without a die and with a die, d = 0.108 mm.

The surface of the reference wires (i.e., those with a diameter of 0.2 mm) was covered with longitudinal scratches, as shown in Fig. 7a, which originated from the drawing die. Such scratches are typical especially when using worn dies. Scratches with a different orientation appeared sporadically due to wire handling during the process. For this wire, the R_a roughness value was approximately 0.12 µm. Microscopic examinations showed that the grains located close to the outer surface of the wire were clearly larger for the material processed by die-free drawing than for the material subjected to the combined die-free and die drawing method. In addition, the wire surfaces were clearly oxidized (Fig. 7b and 7c) after undergoing both processing methods. The oxide layers covered the scratches on these samples; however, the deepest scratches were visible on the surface of the sample obtained by combined die-less and die drawing. Although the surface of the wire after the combined process was less oxidized, the surface scratches were not visible; however, relatively superficial

surface discontinuities were observed, with different orientations relative to the wire axis, as shown in Fig. 7d (Kustra *et al.*, 2023).

The ever-increasing demands on the physical and mechanical properties of metals and alloys require the search for new technical solutions to obtain metal products with improved performance. One of the intensively researched areas is the development of methods and devices for obtaining an ultra-fine grain structure (UFG) using SPD methods on steels. The ECAP and torsion plastic deformation methods, which have become classic, have serious limitations in terms of workpiece size. In addition, the search for innovative solutions to ensure the formation of UFG structures in long workpieces (wires, long thin bars) is one of the directions of development of this new type of technology. Wire, being one of the popular types of metal products, can be used both as a final product of mechanical processing and as a starting material for the production of metal wire ropes, electrodes, and others.

The aim of another study was to apply a combined wire drawing technology, which includes alternating bending and torsion stresses to a C70 steel wire (SR EN ISO 16120-4:2017) with a diameter of 3 mm. The steel has a high carbon content, and its chemical composition is shown in Table 1.

Table 1

Chemical composition (in %) of C70 steel

C	Si	Mn	Ni	S	P	Cr	Cu
0.67-0.75	0.17-0.37	0.5-0.8	< 0.25	< 0.035	< 0.035	< 0.25	< 0.2

To carry out a series of experimental tests, a setup was employed that generated the combined deformations described above (Fig. 8).

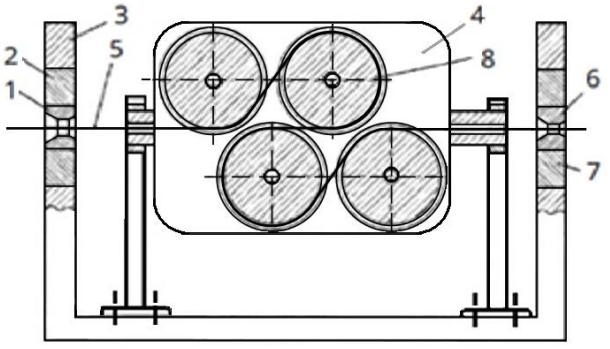

Fig. 8 – Schematic of the installation for combined deformation of wire by drawing with alternating bending and torsion.

The installation consists of the machine housing 3, in which dies 1 and 6 are mounted in supports 2 and 7, respectively. Wire 5 is inserted into die 1 and then passes through the four-roller device 4, which ensures the application

of bending deformation. The four rollers of the device have an independent drive, which ensures their rotation. In this case, the wire is deformed by torsion. The diameter at the first die is 2.86 mm, and at the second die it is 2.75 mm, and the rotation speed of the four-roller device was 150 rpm.

The combination of drawing with bending and torsion is characterized by a complex stress-strain state regime, which involves non-uniform distributions of stresses and strains in the material volume. As a result of this process, a well-defined deformation texture was found in the processed wire, highlighting a marked anisotropy of mechanical properties specific to wire drawing. The information in Table 2 provides a solid basis for the development and improvement of technological processes dedicated to wire manufacturing, allowing the control and adjustment of mechanical properties to pre-established levels, depending on the requirements of the final applications.

Table 2

Results of the Fourier analysis.

Parameter	Original sample	Drawn sample	Drawing sequence, 3.0-2.86-2.75 mm, with bending on rollers with a diameter of 60 mm and torsion at a speed of 150 rpm
Texture direction index	0.706	0.719	0.791
Radial wavelength, μm	9.968	9.968	10.679
Radial wavelength index	0.139	0.139	0.142

Fourier analysis of scanning probe microscopy and surface imaging of high-carbon wire after the drawing process combined with alternating bending and twisting found that spatial parameters (texture direction index, radial wavelength index, and radial wavelength index) can be used for the microscopic characterization of surface anisotropy as shown in Fig. 9 (Polyakova *et al.*, 2023).

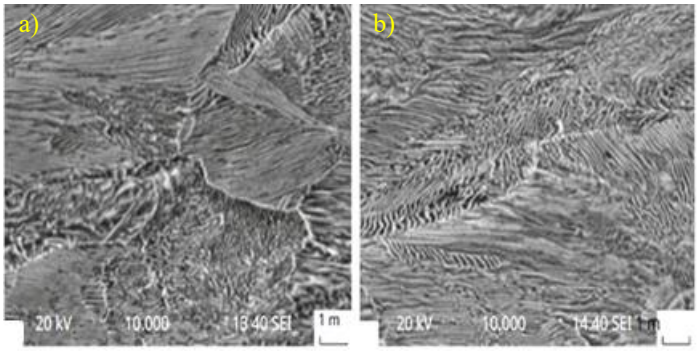

Fig. 9 – Microstructure of steel after different types of deformation processes: a) drawing sequence, 3.0–2.86–2.75 mm; b) combined deformation process through the drawing sequence, 3.0–2.86–2.75 mm with bending on rollers with a diameter of 60 mm and torsion of 150 rpm.

In another study, drawing is also achieved by applying alternating bending and torsion stresses followed by final passage through the die. When designing a new combined deformation method, it is necessary to study the particularities of the influence of different types of deformation on the properties of the wire. Alternating bending is widely used in various metalworking technologies, both as an intermediate operation and as a single operation. In some cases, alternating bending can be used as a processing technique with a specific effect on the structure and properties of the metal without changing the shape of the product. The results obtained can be applied in the practice of designing technologies for manufacturing wires with various cross-sections from different materials. Torsion strongly influences the properties of the deformed metal. This is a type of deformation in which each element of the semi-finished product rotates around the horizontal axis. Torsion is the basic operation in the manufacture of metal wire ropes, so the study of metal properties after torsion is essential for obtaining high-quality metal products. Torsion is characterized by a complex state of stresses and strains, which reaches its maximum value at the surface and tends toward zero at the center of the steel wire. After torsion, the transverse lines on the surface of a round-section workpiece product remain flat, and the diameters of the cross-sections and the distances between them do not change.

In order to evaluate the technological possibilities and constraints of combined plastic deformation on medium carbon steel wire, a comprehensive study was conducted on the influence of processing methods on the microstructure and mechanical properties obtained. For the experiments, a 3.45 mm diameter carbon steel wire with the following chemical composition was selected: 0.5% C; 0.2% Si; up to 0.6% Mn; up to 0.25% Cu; up to 0.08% As; up to 0.25% Ni; up to 0.040% S; up to 0.035% P; up to 0.25% Cr. The aim of the experiment was to identify the effect of different types of plastic deformation (reduction, elongation, and bending) and their combination with torsion on the wire. The reduction ratio was chosen at 37%, depending on the mechanical properties of the wire in its initial state. Bending deformation was applied to the wire as it passed through the 4-roller system, with rollers having a diameter of 90 mm. Torsion deformation was performed at 150 rpm. The combination of drawing, torsion, and bending was achieved using an experimental laboratory assembly.The results for carbon steel wire after different types of deformation processing are shown in Fig. 10. Using computer visualization, 2D images were obtained. In 2D visualization, each point on the surface $Z = f(x, y)$ is identified by a defined color, depending on the height of the point (z-coordinate). The microstructure of medium carbon steel wire consists of ferrite-cementite and a small amount of free ferrite, which is found separately along the boundaries of pearlite colonies as in Fig. 10.

This aspect is characteristic of steel with such a carbon content (the microstructure is uniform). After the drawing process, it can be seen that the

cementite plates become curved in both directions (Fig. 11a, b).

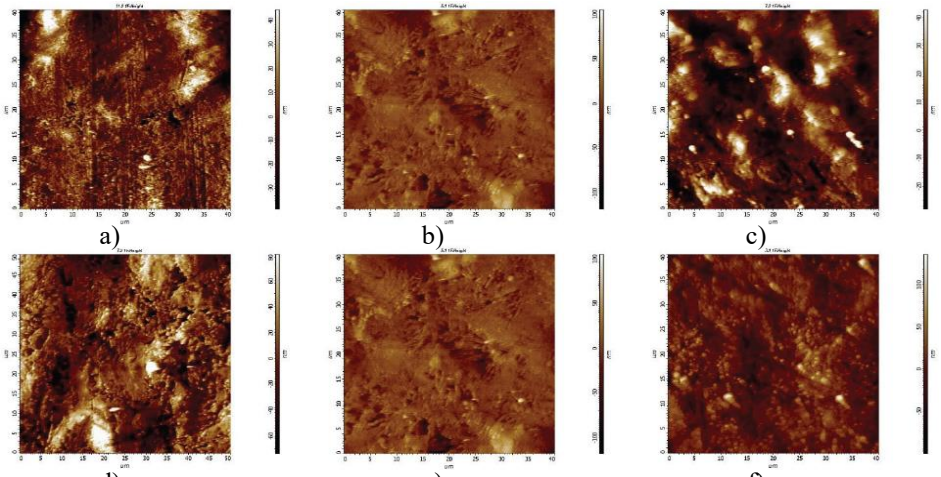

a) b) c)

d) e) f)

Fig. 10 – Microstructures of medium carbon steel wire after drawing (a, d), drawing with bending (b, e), and drawing with bending and twisting (c, f); (a-c – cross section, d-f – longitudinal section).

Combining the drawing process with bending leads to fragmentation of the cementite plates (Fig. 11c, d), which becomes even more pronounced after drawing with bending and torsion (Fig. 11e, f).

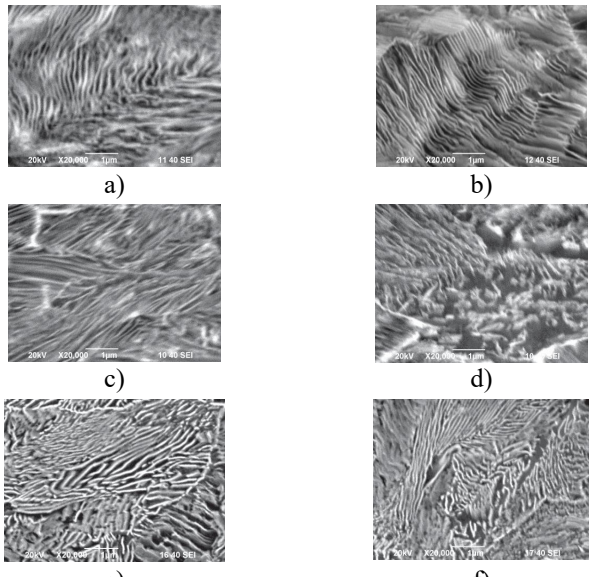

a) b)

c) d)

e) f)

Fig. 11 – Deformation and fragmentation of cementite plates after drawing (a, b); drawing with bending (c, d); drawing with bending and torsion (e, f); (a, c, e - longitudinal section; b, d, f - cross section).

This phenomenon can be explained by the processing of metal within this complex type of plastic deformation action. As a result of combining different types of deformation on medium carbon steel wire, a decrease in all dynamic hardness parameters is observed. This can be explained by the fact that after this type of deformation, the wire becomes more ductile, but at the same time its strength does not decrease as much compared to the drawing process. These particularities of the mechanical properties that medium-carbon steel wire exhibits after combined deformation processing can be very useful for practical applications in steel wire rope manufacturing (Polyakova *et al*., 2017).

Another study analyzed the zinc coating on the surface of medium carbon steel wire C42D (SR EN ISO 16120-2:2017), with a diameter of 5.5 mm, with 7 reduction steps down to a diameter of 2.2 mm, using dies with a drawing angle α = 3, 4, 5, 6, 7° (Table 3). The Johnson-Cook equation is one of the primary constitutive models widely used for metals undergoing large deformation, high strain rates, and high temperatures (Aghdami and Davoodi, 2020). In the galvanized wire drawing process, lubrication conditions affect the structure and properties of the zinc coating on the wire. Fig. 12 shows the significant effect of the die angle and drawing speed on the lubrication conditions. As the drawing speed increases, the amount of lubricant decreases.

Table 3
Wire drawing diagram

Number of draws	0	1	2	3	4	5	6	7
Wire diameter, mm	5.5	4.73	4.1	3.57	3.13	2.77	2.46	2.2
Gp, %	-	26.04	24.86	24.18	23.13	21.68	21.13	20.02
Gc, %	-	26.04	44.43	57.87	67.61	74.64	79.99	84
Individual firing speeds								
v, m/s	-	1.06	1.43	1.9	2.47	3.15	4	5
	-	2.12	2.86	3.8	4.94	6.31	8	10
	-	3.17	4.28	5.7	7.41	9.46	12	15
	-	4.22	5.7	7.59	9.88	12.62	16	20

Note: Gp is single reductions, Gc is total reductions and *v* is the drawing speed.

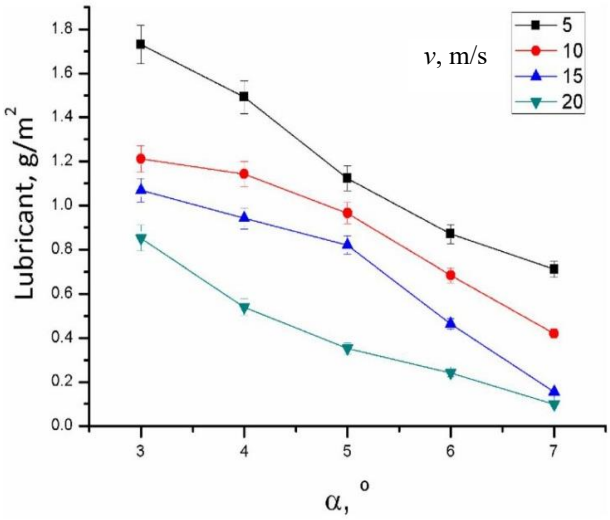

Fig. 12 – Lubricant quantity depending on the die angle and drawing speed.

Wires drawn at a speed of 20 m/s, compared to wires drawn at a speed of 5 m/s, depending on the drawing angle, were characterized by 58.9 to 88.4% less grease (Hwang, 2024, Suliga e*t al.*, 2022).

3. Numerical modeling of wire drawing processes

Modeling the ECAP process of a bimetallic wire

The continuity of deformation is ensured by performing drawing after ECAP. With such a unique deformation pattern, fairly high tensile stresses develop in the cross section of the workpiece, and an incorrect choice of process parameters can lead to wire breakage.

The combined process was developed only for homogeneous materials. The starting material for wire ropes production is often bimetallic wire, which is a long rolled steel product combined with metals and alloys with different chemical and physical characteristics. The implementation and commercialization of the ECAP continuous wire drawing process will enable the production of high-quality bimetallic wires. In this regard, an important task is to study the structural changes in a bimetallic wire during drawing and ECAP and to establish the relationship between the structural states of the material before and after deformation. This will contribute to the understanding of the processes and make it possible to predict the mechanical properties of the wires.

In order to reduce the number of laboratory tests, the deformation of a bimetallic wire was modeled using DEFORM software, which allows the modeling of almost any plastic deformation process. Following the modeling of the combined process (ECAP and wire drawing), the stress-strain state that

occurs for each of the materials when the two operations are applied was analyzed. The starting material was a steel-copper bimetallic wire with a diameter of 10 mm, the diameter of the steel core being 8 mm. The core material was AISI-1016 steel, and the cladding material was CDA 110 copper alloy (commercial copper). The elastoplastic model was chosen as the model for the two materials (core and cladding). Since the materials do not move relative to each other in the bimetallic wire, the interface condition between them is a perfect bond. The friction coefficient between the aluminum cladding and both tools (ECAP die and wire drawing die) was set to 0.1, which corresponds to a polished lubricated surface. The speed at the front and rear ends of the workpiece was 10 mm/sec, and the deformation was performed at room temperature. Figure 13 shows the hardening curves of these materials at a temperature of 20°C extracted from the DEFORM materials database.

The use of these models has demonstrated that the cladding and core can separate at the front end, shown in Fig. 14a, and at the rear end of the workpiece, shown in Fig. 14b. Analysis of the calculated results has established that wire breakage between the ECAP die and the drawing die and separation of the cladding and core can be prevented by adjusting the drawing speed at the front end of the workpiece and the pushing speed at the rear end.

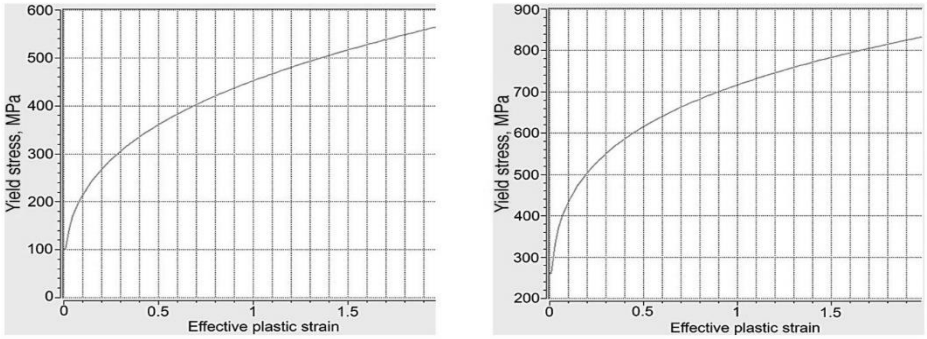

a) b)

Fig. 13 – Hardening curves at 20°C: a) copper CDA 110;
b) steel AISI-1016.

Incorrectly selected kinematic parameters can cause wire breakage or separation of the cladding. For the process to be stable, it is necessary to comply with the condition given by the constant volume law:

$$f_0 v_0 = f_1 v_1, \tag{1}$$

where f_0 and f_1 are the cross-sectional areas of the workpiece before and after passage, respectively; v_0 and v_1 are the speeds of the rear and front ends of the workpiece, respectively.

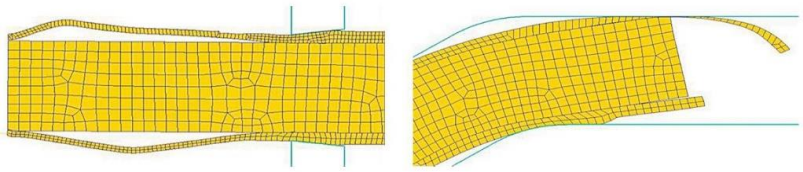

a) b)

Fig. 14 – Separation at the ends of the bimetallic wire:
a) front end; b) rear end.

Thus, if the rear speed is 10 mm/sec and the cross-section of the wire decreases from 10 to 9.5 mm, the front speed must be 11.08 instead of 10 mm/sec. Due to the difference between the front and rear speeds required for a stable combined process, the mold channels are not completely filled in the ECAP stage, which is atypical for conventional pressing as shown in Fig. 15. This effect is achieved by providing a higher speed at the front end of the workpiece (to create tension) than the preset speed of its rear end (which is similar to the action of a press). At the connections of the mold channels, in the transverse direction, there is some tension in the surface layers: the upper half of the cross-section is stretched at the first connection, and the lower half at the second connection. As a result, the thickness of the coating decreases from 1 to 0.96 mm. The thickness of the core does not change at this stage of deformation.

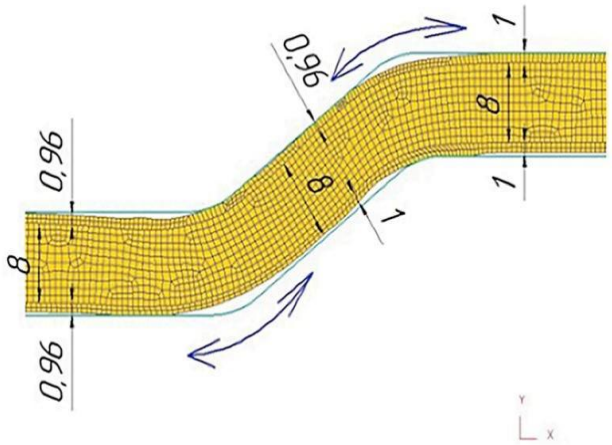

Fig. 15 – Metal deformation during passage
through the inclined channel.

In the ECAP stage of the combined process, the shell and core undergo different deformations when entering the ECAP die channels. The equivalent deformation of the shell is maximum (ε = 1.5) at the channel connections as a result of the displacement and friction of the material with the channel walls (Fig. 16).

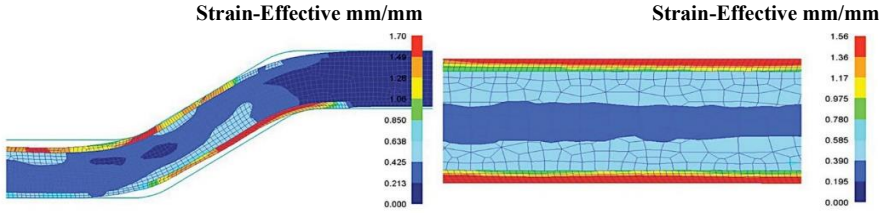

a) b)

Fig. 16 – Equivalent stress: a) ECAP stage; b) drawing stage.

The core undergoes much lower deformation-its central area deforms to $\varepsilon = 0.4$. The surface layers of the core deform more ($\varepsilon = 0.6$). Although both materials are perfectly bonded to each other and should deform equally, their deformation is very different due to their different strength to deformation.

After the drawing stage, the deformation in the shell increases to $\varepsilon = 1.56$. However, the surface stress extends much deeper into the workpiece due to the more intense reduction of the core. As they pass through the ECAP die channels, the shell and core are subjected to different levels of equivalent stress across the entire junction of the channels. The average equivalent stress in the copper shell is 310 to 330 MPa (Fig. 17a). Variable stress distribution depending on sign occurs in the steel core due to pulling at the front end (tension) and pushing at the rear end (compression).

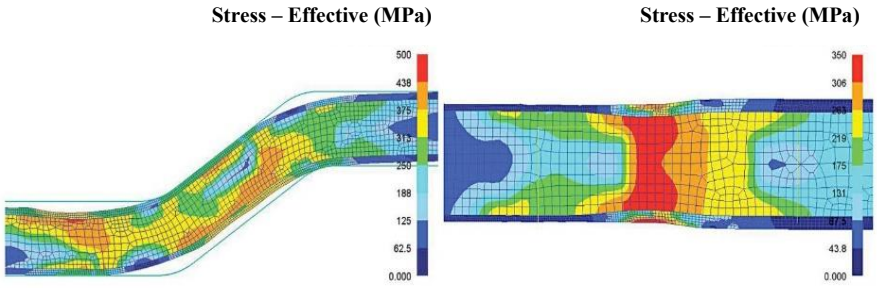

a) b)

Fig. 17 – Equivalent stresses in the copper cladding model:
a) ECAP stage, b) drawing stage.

In the intermediate channel, some stress occurs in the lower part of the core, reaching 480 MPa. In the exit channel, however, where the rear speed is lower, the maximum stress is observed in the upper part of the core (490 MPa), counterbalancing the entire deformation zone. In the drawing stage (Fig. 17b), the deformation zone becomes symmetrical. Due to the higher deformation resistance of copper, the stress distribution across the thickness of the copper cladding is very uneven. In the contact area between the cladding and the

drawing die, the stress is 300 to 310 MPa, gradually decreasing to 220 MPa in the contact area with the core. The equivalent stress in the steel core increases to 350 MPa due to the stronger reduction.

In the laboratory test, a steel-copper wire was drawn in the BI/550 M wire drawing machine. A die with equal channels with a channel diameter of 10 mm and a channel junction angle of 145° was installed in front of the drawing die. The die is located in an oil container. There was a single deformation pass. The starting diameter of the workpiece was 10.0 mm. The carbide dies used had polished channels, reduced taper angles, and smooth transitions between areas. The surface of the bimetallic wire was prepared for drawing following a typical procedure for steel wires, using a mixture of soap and sulfur powders as a lubricant. The wire speed was 10.0 mm/sec in the ECAP die and 13.6 mm/sec in the drawing die.

After each operation, the cross-sectional and longitudinal sections of the samples taken were subjected to metallographic analysis using a Leica bright field microscope. For microstructural analysis, 15 mm long samples were cut from the bimetallic wire and micro-sections were prepared at the ends following a standard procedure. Vickers microhardness was measured using the Leica bright field microscope and a 1 N microhardness tester.

Fig. 18 shows the microstructure of the bimetallic wire after ECAP. It can be seen that the grain size before deformation is 50 μm in the copper coating and 18 μm in the steel core.

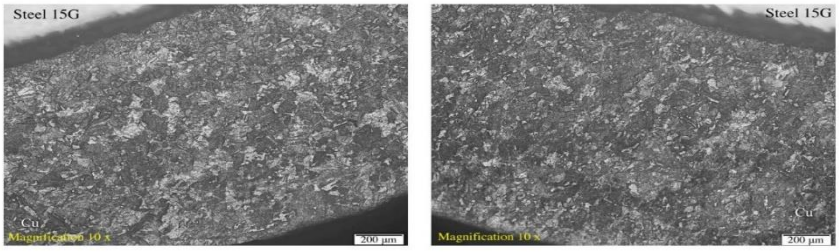

a) b)

Fig. 18 – Microstructure of bimetallic wire: a) before deformation; b) after passing through ECAP die.

It was found that after passing through the ECAP die channels, the initial size of the copper grains decreased to 30–35 μm, and the shape of the grains became equiaxial, which corresponds to the ECAP effect. During drawing, new grains continue to form, their size decreases to 25–30 μm, and there is a certain elongation of the grains in the longitudinal direction, resulting from the tensile stresses in this section.

Analysis of the core microstructure established that after passing through the ECAP die channels, the initial grain size (18 μm) hardly changes,

with only a few grains becoming smaller. In the intermediate zone between the ECAP die and the drawing die, the grain hardly changes. However, there is also some elongation of the grains in the longitudinal direction. Since the core is much thicker than the shell, the microstructure at the exit of the drawing die was examined at two points: in the axial and surface areas. In the surface area, the grain size decreases to 14 μm and the grain shape becomes equiaxial, with an approximately equal surface area. In the axial area, the grain size decreases insignificantly to 17 μm, with the grain shape becoming strongly elongated after the drawing stage (Volokitina *et al.*, 2021).

4. Conclusions

The study concludes that over the last decade, new materials have been developed, especially high-strength steels with multiphase microstructures containing martensite and austenite, belonging to the AHSS (Advanced High Strength Steels) group, as well as non-ferrous alloys with main representatives such as aluminum, magnesium, and titanium.

Recently, studies have been published investigating the effects obtained by combining wire drawing with other operations in which tensile, bending, or twisting stresses are applied to wire products. In general, an increase in the mechanical strength of drawn wires has been observed, but at the same time the plastic properties of the materials have been significantly reduced. Solutions are expected that will allow for increased strength while maintaining acceptable plasticity.

To obtain ultra-thin wires, a process combining die-less drawing with multiple passes of conventional drawing, used alternately in separate passes, was developed, which proved to be relatively easy to control. The increased roughness of the wire obtained during die-less drawing has negative effects, especially when drawing thin wires; however, the roughness can be reduced during the drawing process by subsequently using conventional drawing. This not only allows for a reduction in the achievable wire diameter and control of its surface roughness, but also significantly increases its mechanical strength. The use of such an approach allows the development of a technology for producing ultra-thin wires. The diameter of the brass wire produced was 0.017 mm, which is up to 6 times thinner than a human hair. It is believed to be the thinnest long brass wire currently manufactured in the world. The proposed combined technology can be adapted to the large-scale, economically efficient production of wires with a diameter below that achieved by conventional wire drawing technology.

Other research has confirmed an increase in the strength of steel-aluminum and steel-copper bimetallic wires through SPD. The marked change in microstructure was initiated by combining ECAP with steel-aluminum wire drawing and made it possible to obtain the following relevant results:

- during deformation inside the steel core, fragmentation of ferrite and pearlite is observed in the surface area at 11 μm and in the axial area at 16 μm;

- the strength properties of the wire, even after two deformation passes, increase considerably compared to the initial state. The ultimate tensile strength (σ_f) and yield strength ($\sigma_{0.2}$) doubled, but the relative elongation of the wire decreased by approximately 15.6%.

In the steel-copper wire, microstructural analysis revealed uneven deformation of both layers. The copper coating, with an initial grain size of 50 μm, underwent a reduction in average size to approximately 30 μm. The steel core showed variations in grain size across the cross-section, with an initial size of 18 μm. In the surface layers, the grains were approximately 14 μm, and in the axial area approximately 17 μm, which corresponds to an average size of 16 μm across the entire section. Also, after the drawing stage, the grains show a pronounced elongation as a result of the action of tensile stresses.

Numerical modeling of combined wire drawing processes provides valuable information on stresses, strains, temperature, friction, and material flow. For the finite element model of bimetallic wire drawing, equivalent deformation and equivalent stress were considered as parameters of the stress-strain state. It was found that when the cladding is subjected to high equivalent strain, the core also exhibits significant strain values. The strain distribution was as follows: in approximately 70% of the core diameter, the deformation ranges from 0.35 to 0.39, and in the remaining portion, the values increase to 0.50–0.55. The intensification of the steel core reduction process causes a very uneven distribution of stresses in both materials for all transitions: stresses decrease sharply from the outer layers to the inner layers of the shell. In the core, the stress distribution shows a pronounced gradient and can be represented by a curve with a cup-shaped profile.

REFERENCES

Aghdami A.M., Davoodi B., *An inverse analysis to identify the Johnson-Cook constitutive model parameters for cold wire drawing process*, Mechanics & Industry, 21, 527, (2020), https://doi.org/10.1051/meca/2020070.

Badi R., Bensaada S., Tala-Ighil N., Lebaal N., *Numerical analysis of the effects of incremental reduction rate in the wire drawing process*, The International Journal of Advanced Manufacturing Technology, 133, 5197-5209 (2024), https://doi.org/10.1007/s00170-024-13982-1.

Demin D., Grebenkin I., *Application of ML methods to predict residual stresses and strains after wire drawing process*, The International Journal of Advanced Manufacturing Technology, 133, 3461-3473 (2024), https://doi.org/10.1007/s00170-024-13949-2.

Gronostajski, Z., Pater Z., Madej L., Gontarz A., Lisiecki L., Lukszeka-Solek A., Lucasza J., Mroz S., Muskalski Z., Muzykiewicz W., Pietrzyk M., Sliwa R.E.,

Tomczak J., Wieworowska S., Winiarski G., Zasadzinski J., Ziolkiewicz S., *Recent development trends in metal forming*, Archives of Civil and Mechanical Engineering, 19, 898-941 (2019), https://doi.org/10.1016/j.acme.2019.04.005.

Hwang J.K., *Wire drawing behaviors with die angle and strain hardening rate of a metal.* Journal of Materials Engineering and Performance, 34, 2028-2045 (2024). https://doi.org/10.1007/s11665-024-09180-5.

Kustra P., Wróbel M., Dymek S., Milenin A., *Novel drawing technology for high area reduction manufacturing of ultra-thin brass wires*, Archives of Civil and Mechanical Engineering, 23, 144 (2023), https://doi.org/10.1007/s43452-0230.

Kuznetsov S.A., *Simulations of the drawing process in a system of pressure dies and work dies*, Steel in Translation, 53(12), 1170–1175 (2023), DOI: 10.3103/S0967091223700067.

Polyakova M.A., Gulin A.E., Golubchik E., *Effect of combined tensile, bending and torsion deformation on medium carbon steel wire*, MATEC Web of Conferences, 128, 05007 (2017), https://doi.org/10.1051/matecconf/201712805007.

Polyakova M.A., Pivovarova K.G., Gulin A.E., *Features of texture formation of high-carbon steel wire after combined deformation treatment*, Steel in Translation, 53, 1211-1216 (2023), https://doi.org/10.3103/S096709122470013X.

Renk O., Edalati K., Hohenwarter A., *Saturation of grain fragmentation upon severe plastic deformation: Fact or fiction?*, Advanced Engineering Materials, 26, 2400578 (2024), https://doi.org/10.1002/adem.202400578.

Suliga M., Wartacz R., Michalczyk J., *High speed multi-stage drawing process of hot-dip galvanised steel wires*, The International Journal of Advanced Manufacturing Technology, 120, 7639-7655 (2022), https://doi.org/10.1007/s00170-022-09277-y.

Suliga M.,Wartacz R., Hawryluk M., *Evolution of zinc coatings during drawing process of steel wires*. Archives of Civil and Mechanical Engineering, 23, 120, (2023). https://doi.org/10.1007/s43452-023-00669-9

Truschner M., Pengg J., Loder B., Koberl H., Gruber P., Moshtaghi M., Mori G. , *Hydrogen resistance and trapping behaviour of a cold-drawn ferritic–pearlitic steel wire*, International Journal of Materials Research, 114(6), 439-452 (2023), https://doi.org/10.1515/ijmr-2022-0376.

Volokitina I.E., Naizabekov A.B., Volokitin A.V., *Effect of deformation by ECAP-drawing method on change in steel-aluminum wire properties,* Metallurgist, 66, 9-10 (2023), https://doi.org/10.1007/s11015-023-01436-0.

Volokitina I.E., Naizabekov A.B., Panin E.A. et al., *Effect of ECAP-drawing on the microstructure of a bimetallic wire*, Metallurgist, 65, 7-8 (2021), https://doi.org/10.1007/s11015-021-01214-w.

Weiss V., Kot R.A., *Dieless wire drawing with transformation plasticity*, Wire Journal, 9, 182-189 (1969).

*** a, *Steel wire market size to reach USD 123.23 billion by 2031: Growing construction industry propels. The insight partners*. Available at: https://www.globenewswire.com/news-release/2024/11/22/2985974/0/en/Steel-Wire-Market-Size-to-Reach-USD-123-23-Billion-by-2031-Growing-Construction-Industry-Propels-The-Insight-

Partners.html; accessed on 11.04.2025.
[*]* b, *Steel wire market size, share, and analysis by 2031*, Available at: https://www.theinsightpartners.com/reports/steel-wire-market; accessed on 11.04.2025.
[*]* c, *Primary aluminium production*, Available at: https://international-aluminium.org/statistics/primary-aluminium-production/?publication=primary-aluminium-production&filter; accessed on 11.04.2025.
[*]* d, *Refinery production of copper worldwide from 2000 to 2023*. Available at: https://www.statista.com/statistics/254917/total-global-copper-production-since-2006/, accessed on 11.04.2025.

O RECENZIE ASUPRA STADIULUI ACTUAL AL CERCETĂRILOR PRIVIND TREFILAREA SÂRMELOR

(Rezumat)

Trefilarea sârmei este una dintre cele mai populare tehnologii de obținere a produselor finite, care sunt apoi utilizate în toate sectoarele de producție industrială, începând cu industriile de aparate electrocasnice, automobile, alimentară, construcții și până la domeniul aeronautic. Paralel cu dezvoltarea de noi tehnici de trefilare sunt dezvoltate abordări numerice și empirice pentru a îmbunătăți metodele existente și a dezvolta noi tehnologii de trefilare. Mulți algoritmi numerici inovatori, metode experimentale și contribuții teoretice au fost propuse recent de către cercetătorii din domeniu. Aceste metode sunt axate în principal pe îmbunătățirea deformabilității materialelor, obținerea unor sârme cu rezistențe mecanice crescute, cu o bună calitate a suprafeței, cu tensiuni reziduale minime, accelerarea ciclului de producție, reducerea numărului de operații și performanța de mediu a producției. Scopul acestui studiu este de a rezuma tendințele recente de dezvoltare atât în domeniul numeric, cât și în cel experimental al metodelor convenționale de trefilare, precum și în domeniul metodelor noi de trefilare prin deformare plastică severă (SPD). O atenție deosebită am acordat perioadei 2015-2025 privind progresul dezvoltării metodelor de tragere a materialelor greu de prelucrat pentru aplicații auto și aeronave, aspectelor tribologice care au devenit un subiect de mare atenție și evaluarea impactului ecologic al proceselor de trefilare.